# PHOTONIC GENERATION OF TERAHERTZ WAVES FOR COMMUNICATIONS AND SENSING

Tadao Nagatsuma
*Graduate School of Engineering Science, Osaka University,*
*1-3 Machikaneyma, Toyonaka 560-8531, Japan*
*nagatuma@ee.es.osaka-u.ac.jp*

Keywords: Terahertz, Photonics, signal generation, communication, sensing

Abstract: This paper describes how effectively the photonic signal generation schemes are employed to enhance the performance of terahertz-wave systems such as wireless communication, spectroscopy, and tomographic imaging.

## 1 INTRODUCTION

Research on exploring terahertz (THz) waves, which cover the frequency range from 100 GHz to 10 THz, have lately increased since the nature of these electromagnetic waves is suited to spectroscopic sensing as well as to ultra-broadband wireless communications (Nagatsuma, 2009, 2011). One of the obstacles to developing applications of THz waves is a lack of solid-state signal sources.

For the generation of THz waves, photonic techniques are considered to be superior to conventional techniques based on electronic devices with respect to wide frequency bandwidth, tunability, and stability. Moreover, the use of optical fiber cables enables us to distribute high-frequency (RF) signals over long distances instead of metallic transmission media such as coaxial cables and hollow waveguides.

In this scheme, optical-to-electrical (O-E) converters, or "photodiodes", which operate at long optical wavelengths (1.3-1.55 μm), play a key role, and high output current is required in addition to large bandwidth for practical applications. Recent progress of high-power photodiode technology has accelerated the development of THz-wave system applications (Nagatsuma et al., 2009).

In this paper, we will describe how the photonics technologies are employed in THz-wave systems, showing some of our recent applications, in particular based on based on "continuous wave (CW)" signals, such as wireless communications, spectroscopy and imaging.

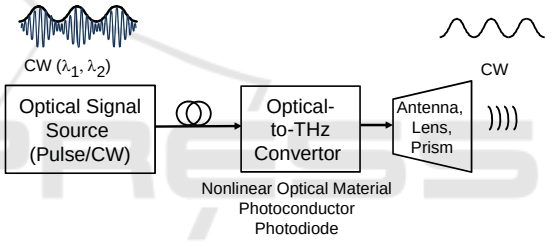


Figure 1: Schematic diagram of photonic continuous-wave THz signal generation.

## 2 GENERATION AND DETECTION OF CONTINUOUS WAVES

In this section, we briefly review schemes for photonic generation and detection of continuous-wave (CW) THz waves.

### 2.1 Signal Generation

Figure 1 shows a schematic of CW THz-signal generation based on optical-to-terahertz conversion. First, intensity-modulated optical signals, whose envelope is sinusoidal at a designated THz frequency, are generated with use of light waves at different wavelengths, $\lambda_1$ and $\lambda_2$. Then, these two-wavelength of lights are injected to conversion media such as nonlinear optical materials (EO), photoconductors (PC), and photodiodes (PD), which



Nagatsuma T.
PHOTONIC GENERATION OF TERAHERTZ WAVES FOR COMMUNICATIONS AND SENSING.
DOI: 10.5220/0004785000430048
In *Proceedings of the Second International Conference on Telecommunications and Remote Sensing (ICTRS 2013)*, pages 43-48
ISBN: 978-989-8565-57-0

leads to the generation of THz waves at a frequency given by

$$f_{RF} = c\Delta\lambda/\lambda^2 \qquad (1)$$

where $\Delta\lambda$ is a difference in wavelength of lights, and c is a velocity of light. The converted signals are finally radiated into free space by an antenna, a lens, etc.

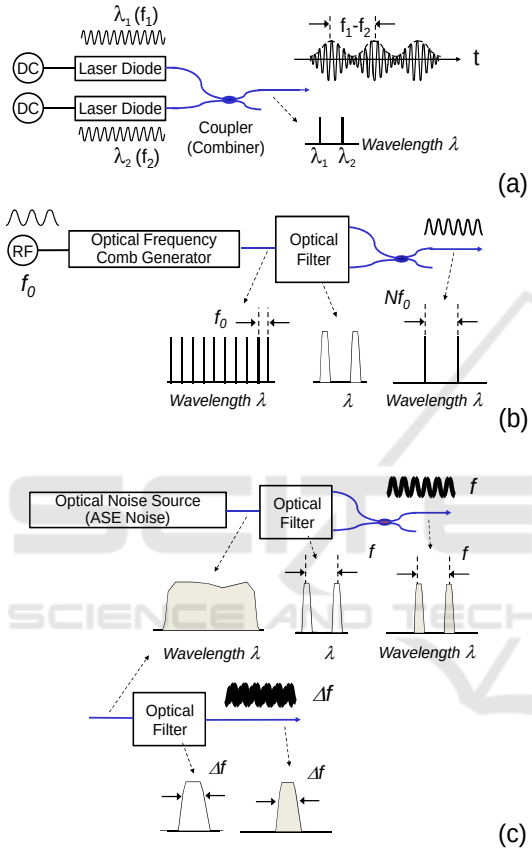


Figure 2: Schematic diagram of optical signal sources.

Typical optical signal sources are depicted in Figs. 2(a) and 2(b); an optical heterodyning technique using two frequency-tunable laser diodes, and using the combination of an optical frequency comb generator and filters, respectively. In the latter case, two wavelength lights are filtered from the optical filters, and this offers us with both wide-band frequency tunability and excellent stability. When so narrow linewidth or frequency resolution in the spectroscopy and/or imaging is not required, we can use two wavelength light filtered from the optical noise source such as ASE noise in optical amplifiers as shown in Fig. 2(c).

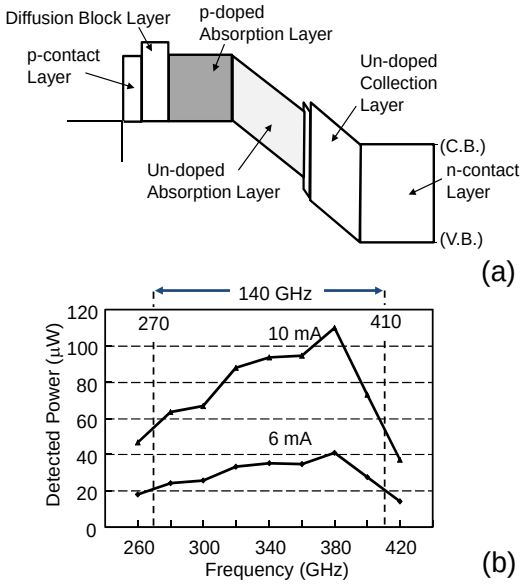


Figure 3: (a) Block diagram of the modified UTC-PD. (b) Output power characteristics.

Among above-memtioned three types of optical-to-electrical conversion media, the photodiode is highly advantageous with respect the conversion efficiency. In addition to the operation at long optical wavelengths (1.3-1.55 μm), large bandwidth and high output current are required for practical applications. Among various types of long-wavelength photodiode technologies, a uni-traveling-carrier photodiode (UTC-PD) and its derivatives have exhibited the highest output powers at frequencies from 100 GHz to 1 THz, with improvement in layer and device structures (Nagatsuma et al., 2009).

Figure 3(a) shows the band diagram of the photodiode optimized for the operation at 300-400 GHz, which is a modification of the UTC-PD. The photodiode chip was packaged into the module with a rectangular waveguide (WR-3) output port (Wakatsuki et al., 2008). Figure 3(b) shows the frequency dependence of the output power generated from the module. The 3-dB bandwidth is 140 GHz (from 270 to 410 GHz), which corresponds to the maximum bit rate of 90 Gbit/s in the case of ASK modulation. The peak output power was 110 μW at 380 GHz for a photocurrent of 10 mA with a bias voltage of 1.1 V. The output power could be further increased to over 500 μW by increasing the photocurrent up to 20 mA with responsivity of 0.22 A/W.

To increase the output power to more than 1 mW, one of the practical approaches is a power-combining technique using an array of photodiodes. With two photodiodes, the output power of >1 mW has been obtained at the photocurrent of 18 mA per photodiode at 300 GHz (Song et al., 2012).

At frequencies of over 300 GHz extending to 1 THz or higher, an antenna-integrated photodiode is more efficient, and semi-spherical silicon lens is often used to collimate a beam radiated from a planar antenna such as bow-tie, log-periodic and dipole antennas (Ito et al., 2005).

## 2.2 Signal Detection

As for detectors, there are several choices in the THz regions, such as "direct detection" using Schottky barrier diodes (SBDs) or bolometers and "heterodyne detection" by combining mixers and local oscillators (Fig. 4). There are electronic and photonic mixers as well as electronic and photonic local oscillators. We choose the best one depending on required performance in each application.

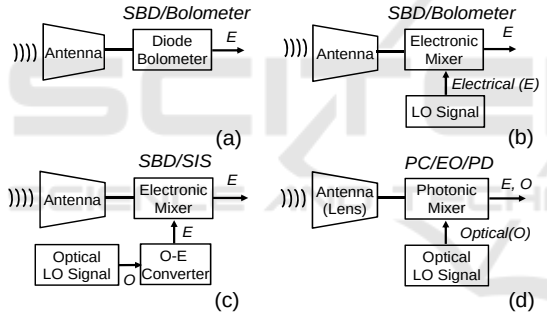


Figure 4: Configurations of THz detection system. O: optical signal, E: electrical signal.

# 3 APPLICATIONS TO COMMUNICATIONS AND SENSING

In this section, we present our recent applications based on based on CW THz signals, such as wireless communications, spectroscopy and imaging.

## 3.1 Wireless Communication

Figure 5 illustrates an example of the application schemes with photonics-based approach, showing how the photonic RF signal generation can be employed together with fiber-optic links (Kleine-Ostmann and Nagatsuma, 2011; H.-J. Song and Nagatsuma, 2011). In addition to the wired link using the light wave at a wavelength of $\lambda_1$, we can transmit the same data with the wireless link by introducing another wavelength ($\lambda_2$) of light wave and mixing the two wavelengths of light in the RF photodiode. The photodiode generates RF signals, whose frequency can be determined the difference in the wavelength of the two light waves, which is given by eq. (1).

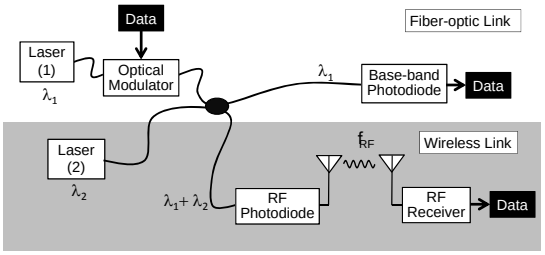


Figure 5: System concept of wired and wireless convergence.

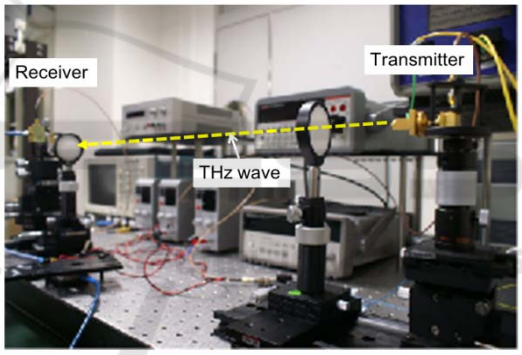


Figure 6: Photo of an experimemtal setup for the wireless link.

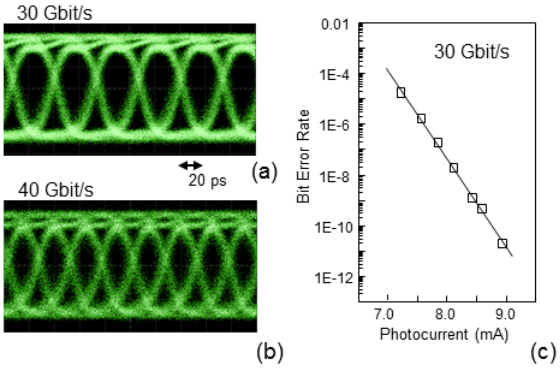


Figure 7: Eye diagrams at 30 Gbit/s and 40 Gbit/s (b), and bit error rate (BER) characteristics at 30 Gbit/s with a carrier frequency of 300 GHz. Photocurrent (horizontal axis of (c)) is proportional to the square root of the transmitted power.

As for the receiver, we can use a simple diode such as a Schottky-barrier diode (SBD) for the demodulation based on the square-law detection in the case of the ASK (OOK) data format. Thus, the receiver becomes more cost-effective and energy-efficient, if we can make use of a wide bandwidth lying over the THz frequency region.

Figure 7 shows transmission characteristics at 300 GHz. For the generation of 300-GHz THz waves, the wavelength difference in two lasers, $\Delta\lambda$, was set to be 2.4 nm, and the optical signal is converted to the RF (THz) signals by the UTC-PD. THz waves are radiated from the horn antenna, and dielectric lenses (2-inch diameter) are used to collimate THz waves for both the transmitter and receiver. The total antenna gain is about 40 dBi. Transmission distance without significant decrease in the received power was typically 0.5 – 1 m.

The performance limitation with respect to the data rate is determined mainly by the bandwidth of the UTC-PD in the transmitter and that of the SBD detector in the receiver. The 3-dB bandwidth of the UTC-PD is 140 GHz (from 270 to 410 GHz), which corresponds to the maximum bit rate of 90 Gbit/s in the case of ASK modulation. While the RF bandwidth of the SBD detector also exceeds 100 GHz, IF (baseband) bandwidth for demodulated signals in the receiver is about 20 GHz, which limits the maximum bit rates. Figures 7(a) and 7(b) shows eye diagrams demodulated by the receiver at 30 Gbit/s and 40 Gbit/s, respectively. From the bit error rate (BER) characteristics, error-free ($BER<10^{-11}$) transmission has been achieved at 30 Gbit/s, which is the highest data rate ever reported for "error-free" wireless links.

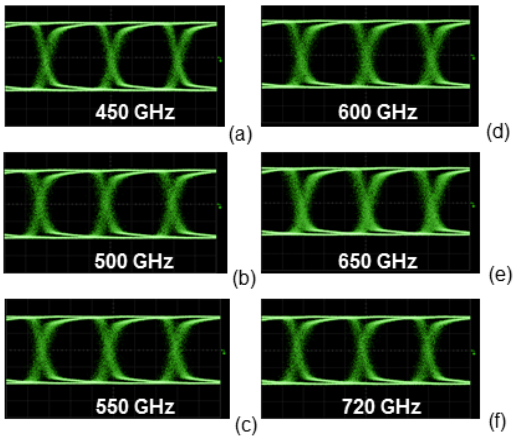


Figure 8: Eye diagrams at the 600-GHz band receiver obtained by changing the carrier frequency or the optical wavelength difference $\Delta\lambda$ from 450 GHz to 720 GHz at a bit rate of 1.6 Gbit/s.

Much larger bandwidth can be ensured when the carrier frequency can be shifted higher. By using antenna-integrated THz UTC-PD module (Ito et al., 2005) together with the 600-GHz band SBD detector (WR-1.5 waveguide), we have increased the available bandwidth of more than 250 GHz with a single transmitter/receiver pair. Figure 8 shows received and demodulated waveforms at carrier frequencies from 450 GHz to 720 GHz. Clear eye diagrams at 1.6 Gbit/s has been obtained, which show error-free transmission over the extremely large bandwidth of 270 GHz.

## 3.2 Spectroscopy

Recently, THz spectroscopy systems based on CW technology, which use monochromatic sources with an accurate frequency control capability, have attracted great interest (Hisatake et al., 2013). The CW source-based systems, referred to as frequency-domain spectroscopy (FDS), provide a higher signal-to-noise ratio (SNR) and spectral resolution. When the frequency band of interest is targeted for the specific absorption line of the objects being tested, FDS systems with the selected frequency-scan length and resolution are more practical in terms of data acquisition time as well as system cost.

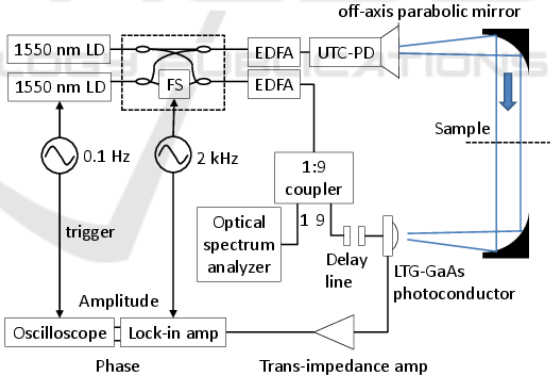


Figure 9: Experimental setup for the frequency-domain spectroscopy. LD: laser diode, EDFA: Erbium-doped fiber amplifier, FS: electro-optic frequency shifter.

THz-FDS system with photonic emitters and detectors is frequently called a homodyne or self-heterodyne system. Figure 9 shows a setup for the THz-FDS system using the UTC-PD for the emitter and a low-temperature-grown (LTG) GaAs photoconductor for the detector. The optical frequency/phase shifter (FS) enables us to accurately measure both the amplitude and phase. Since two

laser diodes (LDs) are free-running, we monitor each wavelength by the optical spectrum analyzer or the wave meter. Figure 10 shows a photo of the experimental setup for the spectroscpoy.

In order to check the frequency accuracy of the system, we measured the absorption line of the water vapor at 557 GHz as shown in Fig. 11. Currently, the experimental standard deviation of the mean for the absorption frequency is about 70 MHz.

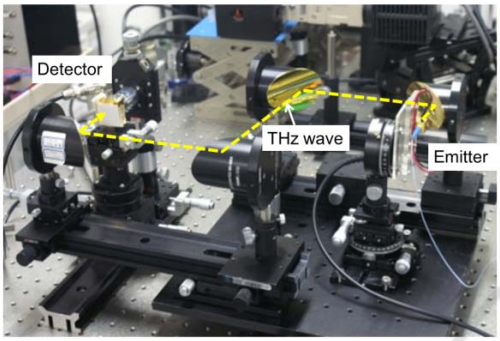


Figure 10: Photo of an experimemtal setup for the spectroscopy.

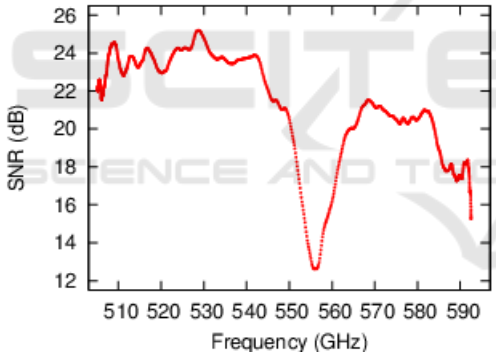


Figure 11: Measured absorption line of the water vapor at 557 GHz.

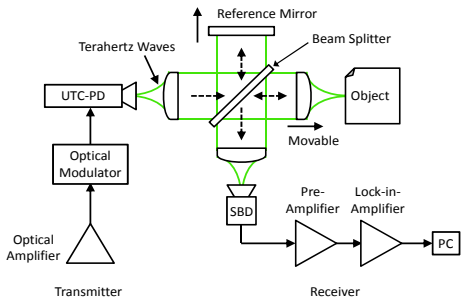


Figure 12: Block diagram of the tomography system using the broadband THz noise signals.

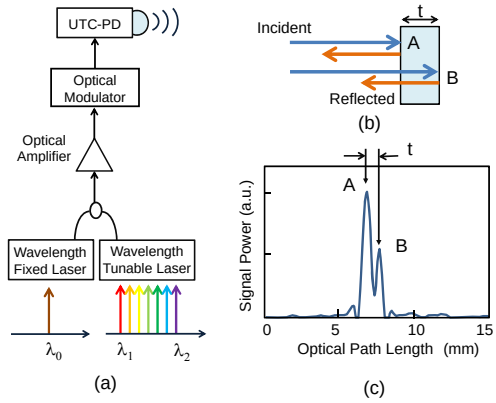


Figure 13: (a) Frequency-swept signal source. (b) Reflection of THz waves at front-side (A) and back-side (B). (c) Point spread function measured with the 600-GHz band system showing the reflection points A and B of a 0.5-mm thick plastic plate.

## 3.3 Imaging

Figure 12 shows a block diagram of the tomographic imaging system using a broadband terahertz noise (incoherent signal) sources and a Mickelson interferometer (Isogawa et al., 2012). This configuration is similar to that of the optical coherence tomography. The broadband noise signals with sufficient power are generated by feeding the amplified spontaneous emission (ASE) noise from the Er-doped fiber amplifier to the photodiode.

In the setup, first, a THz wave travels to the beam splitter after being collimated by a dielectric lens. The beam splitter divides the THz wave into two directions with a power ratio of 50/50. One goes to the reference mirror and the other to an object after being focused. Both reflected waves travel back to the beam splitter again and go to the SBD as a power detector. Finally, detected signals are amplified by a preamplifier and a lock-in amplifier. A personal computer (PC) controls positions of both the reference mirror and the objective lens. The noise bandwidth of 120 GHz centered at 350 GHz determines the depth resolution of 1.2 mm (Isogawa et al., 2012).

In place of the optical noise sources, the combination of a fixed wavelength laser and a wavelength tunable laser (Fig. 13(a)) enables us to modify the tomography system from time-domain to frequency-domain one (Ikeou et al., 2012). In this scheme, depth-position information can be obtained by Fourier-transforming the frequency-(wavelength-) swept interference signals. Figure

13(c) shows the point spread function, which corresponds to the position of the reflection points at A (front-side) and B (back-side) for a plastic plate with 0.5-mm thickness, when the 600-GHz band system was used.

## 4 CONCLUSIONS

We have described system applications, which efficiently take advantages of photonics-based ultra-broadband signal generation techniques at over 100-GHz frequencies. Use of optical fiber cables also makes it easy to handle high-frequency signal distribution or cabling in the instrumentation. These features will not be replaced with electronic systems, even though the operation frequency of electronic devices is increasing up to the THz region.

## ACKNOWLEDGEMENTS

The author wish to thank Drs H. -J. Song, K. Ajito, N. Kukutsu, S. Kuwano, J. Terada, N. Yoshimoto, and T. Ishibashi with NTT, S. Hisatake, M. Fujita, K. S. Horiguchi, Y. Minamikata, T. Ikeou, H. Nishii with Osaka University for their collaboration and support. This work was supported in part by the JST-ANR WITH program and by the Ministry of Education, Science, Sports and Culture, Grant-in-Aid for Scientific Research (A), 23246067, 2011.

## REFERENCES

Hisatake, S., Kitahara, G., Ajito, K., Fukada, Y., Yoshimoto, N., Nagatsuma, T., 2013. *Phase-sensitive terahertz self-heterodyne system based on photodiode and low-temperature-grown GaAs photoconductor at 1.55 μm*. IEEE Sensors Journal, vol. 13, no. 1, pp. 31–36.

Ikeou, T., Isogawa, T., Ajito, K., Kukutsu, N., Nagatsuma, T., 2012. *Terahertz imaging using swept source optical-coherence-tomography techniques.* Tech. Dig. IEEE Intern. Topical Meeting on Microwave Photonics, Session 8, Noordwijk.

Ito, H., Furuta, T., Nakajima, F., Yoshino, K., Ishibashi, T., 2005. *Photonic generation of continuous THz wave using uni-traveling-carrier photodiode.* IEEE J. Lightwave Tech., vol. 23, no. 12, pp. 4016–4021.

Isogawa, T., Kumashiro, T., Song, H.-J., Ajito, K., Kukutsu, N., Iwatsuki, K., Nagatsuma, T., 2012. *Tomographic imaging using photonically generated low-coherence terahertz noise sources.* IEEE Trans. Terahertz Science and Tech., vol. 2, no. 5, pp. 485–492.

Kleine-Ostmann, T., Nagatsuma, T., 2011. *A review on terahertz communications research. J. Infrared Milli. Terhz. Waves*, vol. 32, no. 2, pp. 143–171.

Nagatsuma, T, Ito, H., Ishibashi, T., 2009. *High-power RF photodiodes and their applications.* Laser Photon. Rev., vol. 3, no. 1-2, pp. 123–137.

Nagatsuma, T., 2009. *Generating millimeter and terahertz waves*. IEEE Microwave Magazine, vol. 10, no. 4, pp. 64–74.

Nagatsuma, T., 2011. *Terahertz technologies: present and future,* IEICE Electron. Express, vol. 8, no. 14, pp. 1127–1142.

Song, H.-J., Nagatsuma, T., 2011. *Present and future of terahertz communications.* IEEE Trans. Terahertz Science and Technology, vol.1, no. 1, 256–264.

Song, H.-J., Ajito, K., Muramoto, Y., Wakatsuki, A., Nagatsuma, T., Kukutsu N., 2012. *Uni-travelling-carrier photodiode module generating 300 GHz power greater than 1 mW*. IEEE Microwave and Wireless Components Letters, vol. 22, no. 7, pp. 363–365.

Wakatsuki, A., Furuta, T., Muramoto, Y., Yoshimatsu, T., Ito, H., 2008. *High-power and broadband sub-terahertz wave generation using a J-band photomixer module with rectangular-waveguide output port.* Proc. Int. Conf. on Infrared, Millimeter, and Terahertz Waves, pp. 1999-1–1999-2.